

EST64454: a Highly Soluble σ_1 Receptor Antagonist Clinical Candidate for Pain Management

José Luis Díaz, Mónica García, Antoni Torrens, Ana María Caamaño, Juan Enjo, Cristina Sicre, Adriana Lorente, Adriana Port, Ana Montero, Sandra Yeste, Inés Álvarez, Miquel Martín, Rafael Maldonado, Beatriz de laPuente, Alba Vidal-Torres, Cruz Miguel Cendán, José Miguel Vela, and Carmen Almansa*



Cite This: <https://dx.doi.org/10.1021/acs.jmedchem.0c01575>



Read Online

ACCESS |



Metrics & More



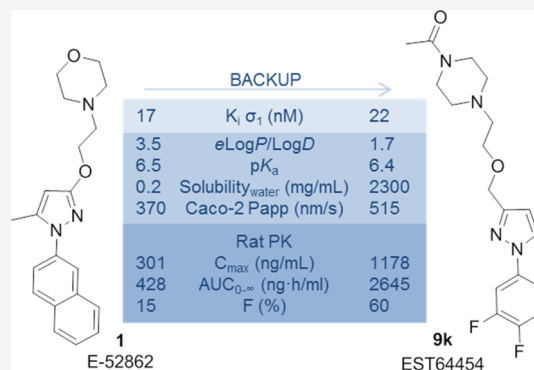
Article Recommendations



Supporting Information

ABSTRACT: The synthesis and pharmacological activity of a new series of pyrazoles that led to the identification of 1-(4-(2-((1-(3,4-difluorophenyl)-1H-pyrazol-3-yl)methoxy)ethyl)piperazin-1-yl)ethanone (**9k**, EST64454) as a σ_1 receptor (σ_1 R) antagonist clinical candidate for the treatment of pain are reported. The compound **9k** is easily obtained through a five-step synthesis suitable for the production scale and shows an outstanding aqueous solubility, which together with its high permeability in Caco-2 cells will allow its classification as a BCS class I compound. It also shows high metabolic stability in all species, linked to an adequate pharmacokinetic profile in rodents, and antinociceptive properties in the capsaicin and partial sciatic nerve ligation models in mice.

BACKUP			
17	$K_i \sigma_1$ (nM)	22	
3.5	eLogP/LogD	1.7	
6.5	pK _a	6.4	
0.2	Solubility _{water} (mg/mL)	2300	
370	Caco-2 Papp (nm/s)	515	
Rat PK			
301	C _{max} (ng/mL)	1178	
428	AUC _{0-∞} (ng·h/mL)	2645	
15	F (%)	60	



INTRODUCTION

The adequate management of pain is still an unmet medical need because currently available treatments provide in many cases only modest improvements, leaving many patients unrelieved¹ and causing a heavy socioeconomic burden.² Currently approved pain therapies such as opioid agonists, nonsteroidal anti-inflammatory drugs, calcium channel modulators, and antidepressants show an efficacy limited by a variety of secondary effects that can preclude their prolonged use. In order to identify analgesic agents with an alternative mechanism of action, we have been working for many years in developing sigma-1 receptor (σ_1 R) antagonists.³

The σ_1 R is a 24 kDa protein of 223 amino acids anchored to the endoplasmic reticulum (ER) and plasma membranes.⁴ It is structurally different from other target classes because it has no direct downstream signaling, and instead, it acts as a molecular chaperone modulating the functions of diverse proteins.⁵ A wide range of evidence is now available to support the role of the σ_1 R in the treatment of pain,³ including potentiation of opioid receptor-mediated analgesia by σ_1 R antagonists⁶ and the fact that σ_1 R knockout mice (σ_1 R-KO)⁷ did not develop pain behaviors after the nerve sensitization developed under neuropathic pain conditions or after capsaicin or formalin injection. The use of σ_1 R antagonists reinforced these findings and was the basis for the selection of S1RA (E-52862, **1**, Figure 1)⁸ as a clinical candidate for the treatment of different pain types. These included chemotherapy-induced neuropathy,

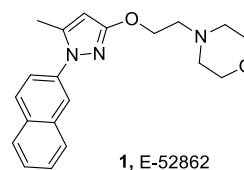
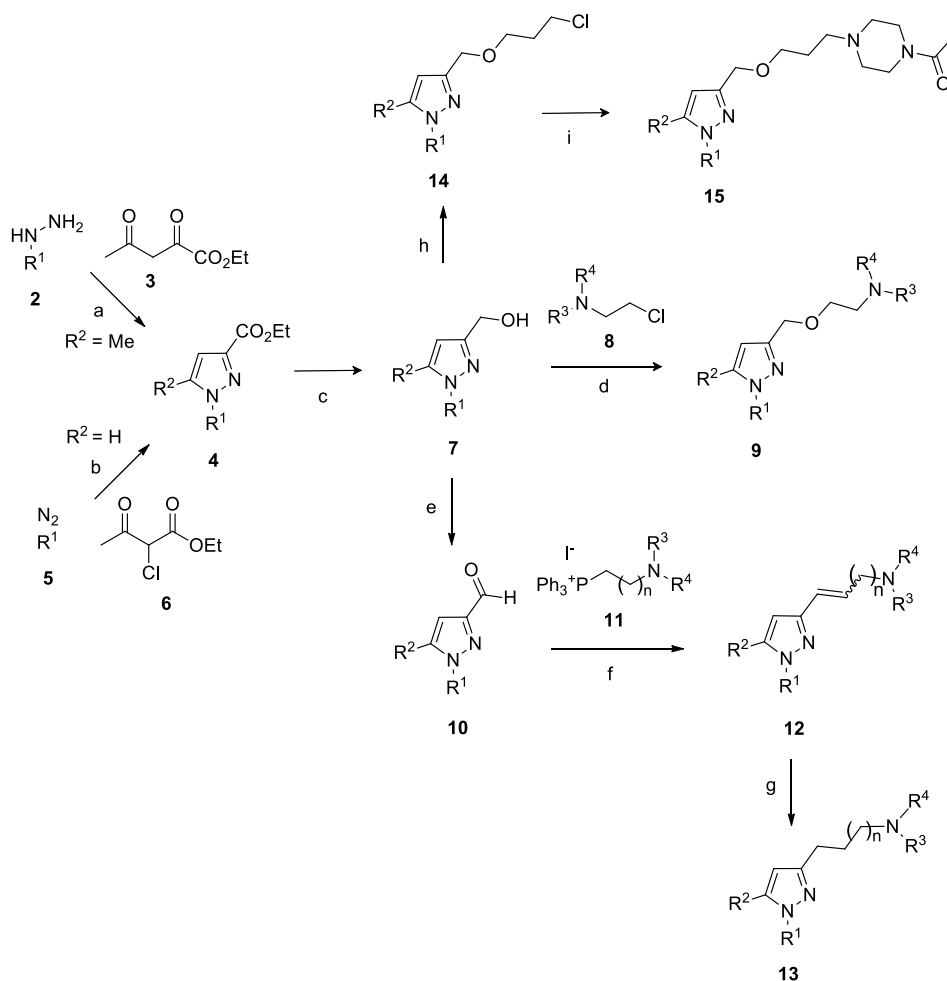


Figure 1. Structure of the σ_1 R antagonist E-52862 (**1**).

where **1** showed a promising reduction in pain scores.⁹ An enhancement of the benefit–risk ratio of the opioid morphine overall clinical profile was also obtained in a clinical trial of postoperative pain due to abdominal hysterectomy.¹⁰

As a backup program, we explored the variation in the morpholine-containing chain of **1**, by elongation of the distance of the O-atom to the pyrazole ring or its replacement by carbon atoms. We thought that these changes could still comply with Glennon's σ_1 R pharmacophore,¹¹ the model used for the development of **1**, and lead to the improvement of some of its properties while maintaining selectivity over the sigma-2 receptor (σ_2 R). The two sigma receptors, σ_1 and σ_2 ,

Received: September 9, 2020

Scheme 1^a

^aReagents and conditions: (a) AcOH, 120 °C; (b) (i) NaOAc, EtOH, rt, (ii) bicyclo[2.2.1]hepta-2,5-diene, Et₃N, toluene, 80 °C, and (iii) xylenes, 135 °C; (c) NaBH₄, EtOH, 80 °C; (d) NaH, THF, 70 °C; (e) MnO₂, CH₂Cl₂, 40 °C; (f) KO^tBu, THF, rt; (g) PtO₂, H₂, MeOH, rt; (h) 1-bromo-3-chloropropane, Bu₄NSO₄H, NaOH, toluene, rt; and (i) 1-acetylpiperazine, DIPEA, NaI, DMF, 90 °C.

have different molecular weights, tissue distributions, and subcellular locations and were initially classified based on their different behaviors in the presence of (+)-pentazocine in rat liver and kidney membranes. Initial assays involved binding on guinea pig membranes, applied to the σ_1 R¹² or to the σ_2 R.¹³ The σ_1 R was cloned soon enough,¹⁴ but the identification of the σ_2 R has been troublesome.¹⁵ Although it was later on proposed to be a part of the progesterone receptor membrane component 1 (PGRMC1),¹⁶ this was ruled out mainly based on the fact that overexpression or knockdown of PGRMC1 failed to affect prototypic σ_2 R ligand binding. The receptor was finally isolated using classical affinity purification approaches¹⁷ and it was identified as the ER-resident membrane protein TMEM97, also known as MAC30. Both TMEM97 and the classical σ_2 R binding site show similar characteristics and behaviors for a range of prototypic σ_2 R ligands.

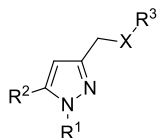
The backup program reported here was directed at finding an alternative derivative to the compound **1** that could improve some of its properties. First, **1** showed an acceptable, but suboptimal, aqueous solubility (0.2 mg/mL) that could be probably improved by reducing its lipophilicity (eLog *P* = 3.5), taking into account the inverse relationship of solubility with clog *P*.¹⁸ Reducing lipophilicity while maintaining good affinity for the σ_1 R and selectivity versus other targets was not

considered a trivial task because polar groups are poorly tolerated in the highly hydrophobic σ_1 R and need to be placed at very specific positions.¹⁹ However, it was worth to be pursued because such a reduction would be also beneficial for the improvement of the overall safety profile. It is well known that decreasing lipophilicity is linked to reduced attrition and promiscuity²⁰ and even a cutoff value of clog *P* = 3 has been proposed to increase the likelihood of not finding toxic events in so-called Pfizer's 3/75 rule.²¹ On the other hand, the exposure of the compound **1** in rodents (with AUC 958 and 428 ng/mL and bioavailability of 34 and 15% after oral administration of 10 mg/kg to mice and rats, respectively) could be improved in order to better establish efficacy–safety ratios along the compound development. With these objectives in mind, we initiated the synthesis and structure–activity relationship (SAR) study that allowed the identification of 1-(4-(2-((1-(3,4-difluorophenyl)-1*H*-pyrazol-3-yl)methoxy)-ethyl)piperazin-1-yl)ethanone **9k** as a selective σ_1 R antagonist clinical candidate for the treatment of pain.²²

CHEMISTRY

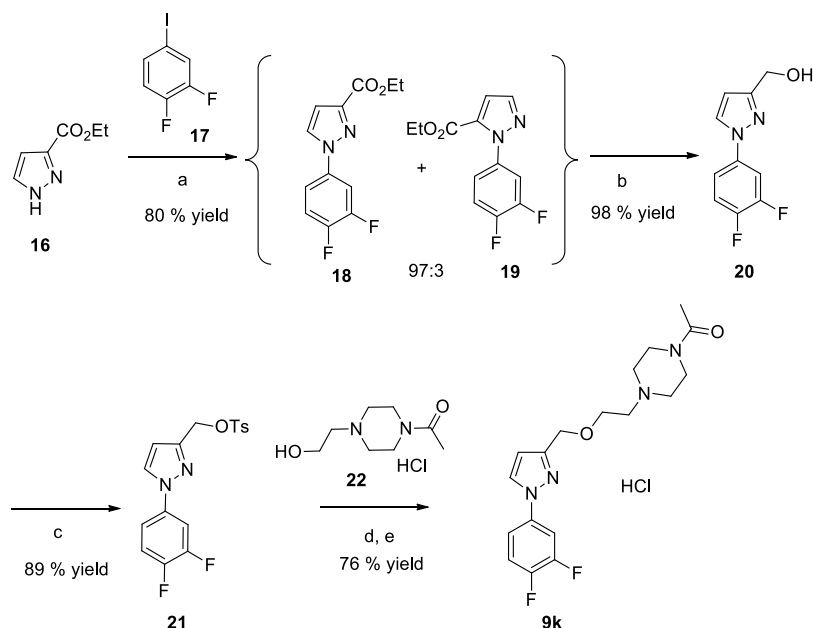
As outlined in Scheme 1, the synthesis of the new pyrazoles **9**–**15** was carried out using three alternative procedures from 3-hydroxymethylpyrazoles **7**. The process started by constructing

Table 1. SAR Data around the 1,3,5-Trisubstituted Pyrazoles



comp	X	R ¹	R ²	R ³	K _i σ ₁ R ^a (h, nM)	K _i σ ₂ R ^b (h, nM)	clog P ^c	hERG ^d IC ₅₀ (nM)
1					17 ± 7	>1000 ^e	3.9	>10,000 ^f
9a	O(CH ₂) ₂	naphthalen-2-yl	Me	morpholyn-4-yl	209 ± 57	>1000 ^e	3.6	NT ^g
9b	O(CH ₂) ₂	3,4-dichlorophenyl	Me	morpholyn-4-yl	14 ± 1	399 ± 76	3.8	NT ^g
9c	O(CH ₂) ₂	3,4-dichlorophenyl	H	morpholyn-4-yl	2 ± 0.2	137 ± 47	3.6	NT ^g
9d	O(CH ₂) ₂	cyclopentyl	Me	morpholyn-4-yl	240 ± 38	>10,000 ^f	2.0	NT ^g
9e	O(CH ₂) ₂	3,4-dichlorophenyl	Me	pyrrolidin-1-yl	6 ± 2	27 ± 1	4.5	5123
9f	O(CH ₂) ₂	3,4-dichlorophenyl	Me	piperidin-1-yl	2 ± 0.3	28 ± 19	5.1	NT ^g
9g	O(CH ₂) ₂	3,4-dichlorophenyl	Me	(2S,6R)-2,6-dimethylmorpholin-4-yl	3 ± 1	180 ± 38	4.8	NT ^g
9h	O(CH ₂) ₂	3,4-dichlorophenyl	Me	4-acetylpiperazin-1-yl	15 ± 0.1	>1000 ^e	3.3	>10,000 ^f
9i	O(CH ₂) ₂	3,4-dichlorophenyl	Me	piperazin-1-yl	278 ± 12	NT ^g	3.4	NT ^g
9j	O(CH ₂) ₂	3,4-difluorophenyl	Me	4-acetylpiperazin-1-yl	58 ± 6	>10,000 ^f	2.5	>10,000 ^f
9k	O(CH ₂) ₂	3,4-difluorophenyl	H	4-acetylpiperazin-1-yl	22 ± 3	>10,000 ^f	2.0	>10,000 ^f
13a	(CH ₂) ₂	3,4-dichlorophenyl	Me	morpholyn-4-yl	5 ± 0.4	232 ± 100	4.2	NT ^g
13b	(CH ₂) ₃	3,4-dichlorophenyl	Me	morpholyn-4-yl	9 ± 1	116 ± 20	4.7	NT ^g
15	O(CH ₂) ₃	3,4-dichlorophenyl	Me	4-acetylpiperazin-1-yl	9 ± 0.1	>1000 ^e	3.6	4084

^aBinding affinity (K_i , nM) to human in transfected HEK-293 membranes using [³H](+)-pentazocine as a radioligand. Each value is the mean \pm SD of two determinations. The K_i values (nM) in this assay for some standard reference compounds are as follows: (+)-pentazocine, 12 ± 1 ; haloperidol, 2 ± 1 ; and DTG, 59 ± 7 . ^bBinding affinity (K_i , nM) to σ_2 R in guinea pig brain membranes using [³H]di-o-tolylguanidine as a radioligand. Each value is the mean \pm SD of two determinations. The K_i values (nM) in this assay for some standard reference compounds are as follows: (+)-pentazocine, 719 ± 63 ; haloperidol, 22 ± 1 ; and DTG, 23 ± 11 . ^c $\log P$ was calculated using ChemDraw. ^dWhole-cell patch clamp hERG blockade. ^eLess than 50% inhibition at $1 \mu\text{M}$. ^fLess than 50% inhibition at $10 \mu\text{M}$. ^gNot tested.

Scheme 2^a

^aReagents and conditions: (a) CuI, Cs₂CO₃, TMEDA, MeCN, 85 °C; (b) LiBH₄, THF, 70 °C; (c) TsCl, KOH, THF, rt; (d) NaH, THF, rt; and (e) HCl, IPA, 0 °C.

the ester derivatives **4**, which were prepared by two different procedures depending on their substitution pattern. Using one of the most prevalent methods for obtaining pyrazoles, that is, cyclization of 1,3-diketones with hydrazine derivatives,²³ the reaction of ethyl acetopyruvate (**3**) with hydrazines **2** afforded the 5-methyl-pyrazoles (**4**, R² = Me) with excellent yields. An alternative method was used for the synthesis of 5-*H*-pyrazoles

(4, $R^2 = H$) involving the reaction of diazonium salts **5** with ethyl 2-chloroacetoacetate (**6**). This reaction proceeded through an intermediate arylhydrazonoyl chloride²⁴ that underwent a [3 + 2] cycloaddition with bicyclo[2.2.1]hepta-2,5-diene, followed by a retro Diels–Alder reaction in refluxing xylenes.²⁵ Reduction of derivatives **4** with NaBH₄ led to the key 3-(hydroxymethyl)pyrazoles **7**, which were alkylated with

chloroethylamine derivatives **8** using NaH in refluxing tetrahydrofuran (THF) to give pyrazoles **9a–h** with moderate to good yields. The derivative **9i** (Table 1) was obtained by deprotection of **9h** with HBr in AcOH, as described in the experimental part. Alternatively, alcohols **7** were oxidized with MnO₂ to afford aldehydes **10**, which were reacted with phosphonium salts **11** to render alkenes **12**. Reduction of **12** using PtO₂ under a H₂ atmosphere afforded the alkylated pyrazoles **13** with good yields. Furthermore, a derivative with an extended alkyl chain was synthesized from **7** by alkylation with 1-bromo-3-chloropropane and subsequent substitution with 1-acetypiperazine, affording the pyrazole **15** with moderate yield.

As an alternative synthesis for the large-scale production of **9k**, the route described in Scheme 2 was developed.²⁶ It is well known that diazonium salts are explosive and their precursor anilines are genotoxic.²⁷ As a consequence, processes avoiding their use are strongly preferred. Furthermore, the yield of the final alkylation was difficult to reproduce when performing the reactions in a bigger scale and needed further improvement. An Ullmann-type reaction was envisaged for the synthesis of 3-(ethoxycarbonyl)-pyrazole **18**, based on the existing literature describing the synthesis of pyrazoles using this methodology.²⁸ Optimization of the reaction conditions included testing of different copper salts as Cu₂O and CuI; solvents such as toluene, DMA, NMP, MeOH, DMF, THF, MeCN, and dioxane; bases such as K₃PO₄, Cs₂CO₃, K₂CO₃, Na₂CO₃, NaHCO₃, and NaOH; and ligands such as bipyridine, 1,10-phenanthroline, ethane-1,2-diamine, N¹,N²-dimethylethane-1,2-diamine, (1*R*,2*R*)-cyclohexane-1,2-diamine, (1*R*,2*R*)-N¹,N²-dimethylcyclohexane-1,2-diamine, TMEDA, and 2-hydroxybenzaldehyde oxime. We observed no difference in the reaction outcomes when using CuI or Cu₂O and that reactions performed in THF or MeCN showed full conversion and cleaner crude products compared to the other tested solvents. Finally, the best base/solvent combination was found to be Cs₂CO₃/MeCN and the best ligand was TMEDA because its use afforded good conversions and minimized byproduct formation. The optimized conditions led to the formation of **18** in an excellent yield and with high regioselectivity (97:3), obtaining only traces of the 5-substituted pyrazole **19**. Reduction of the regioisomeric mixture was performed with LiBH₄ to give 3-(hydroxymethyl)-pyrazole **20**, which was obtained as a single regioisomer after crystallization of the reaction mixture. An alternative alkylation method in relation to that used in Scheme 1 was also envisaged in order to avoid the variability previously observed. Derivatization to the tosyl derivative **21** followed by substitution with the alkoxide of alcohol **22** afforded the pyrazole **9k** in good yields. In this reaction, the hydrochloride salt of the alkylating agent was directly used to afford the final compound as hydrochloride salt, which was the form selected for development. Overall, the process depicted in Scheme 2 allows the synthesis of **9k** with improved efficiency, applying reaction conditions suitable for large-scale production, without the need of chromatographic purification throughout the whole process and using easily available, nontoxic starting materials.

RESULTS AND DISCUSSION

The new compounds synthesized were tested in a primary σ_1 R binding assay using [³H]-(+)-pentazocine⁸ as a radioligand in human transfected HEK-293 membranes and in σ_2 R in guinea

pig membranes using [³H]-di-*o*-tolylguanidine¹³ as a radio-ligand. The active and selective compounds were assayed for the blockade of the human ether-a-go-go-related gene (hERG), an off-target related to cardiac toxicity²⁹ that has been a repeated issue in our previous σ_1 R programs, particularly in structurally related compounds.^{8,26} The results are shown in Table 1.

The SAR was initiated with the preparation of the direct elongated analogue of the reference compound **1**, derivative **9a**, which showed a decrease in σ_1 R binding. Changing the naphthalenyl group by one of the best alternatives identified in previous studies,^{8,30} the 3,4-dichlorophenyl ring, provided an increased affinity (**9b**) but a reduction in selectivity for the σ_2 R. A similar profile was obtained with the unsubstituted derivative in position 2, **9c**. Replacement of the aromatic ring in position 1 with a saturated cyclopentyl ring (**9d**) provided a decrease in affinity.

Replacement of the morpholine ring by other basic groups was investigated over the 1-(3,4-dichlorophenyl)-2-methylpyrazoles. Using more lipophilic cyclic amines, such as pyrrolidine (**9e**), piperidine (**9f**), or dimethyl morpholine (**9g**) provided low nanomolar affinities but was detrimental in relation to selectivity versus the σ_2 R, in agreement with previous findings.³⁰ Introducing a 4-acetypiperazine ring was favorable because the compound **9h** maintained a good activity for the σ_1 R and a good selectivity versus the σ_2 R and was devoid of hERG inhibition. Its naked piperazine counterpart **9i** was substantially less active. Elongation of the acetyl group to bulkier groups was also studied, but either selectivity versus the σ_2 R was impaired or hERG inhibition started to appear (results not shown). In a similar way, elongation of one carbon atom of the linker chain provided the compound **15**, which was interesting in terms of primary affinities, but showed a hERG inhibition IC₅₀ of around 4 μ M.

Replacement of the oxygen-containing linker chain with an alkylidene linker provided compounds **13a** and **13b**, with good σ_1 R affinities but low selectivity. Overall, it seems that selectivity versus the σ_2 R is more easily achieved with more polar compounds, which is consistent with previous results.^{8,30}

More analogues were prepared maintaining a 4-acetypiperazin-1-ylethoxymethyl linker and changing the nature of the aromatic substituents of the phenyl ring in position 1 and keeping methyl or hydrogen in position 2. Compounds **9h**, **9j**, and **9k** emerged as the most interesting derivatives because they showed good affinity for the σ_1 R and good selectivity and were devoid of hERG inhibition.

The compound **9k** was selected for further progression because in addition to its good activity profile, it showed the lowest clog *P*, almost 2 log units below that of the reference compound **1**, which was corroborated by the experimental values (log *P*/log *D*_{7.4} 1.7 for **9k** and 3.5 for **1**). This reduction translated into an exceptionally high thermodynamic solubility both at pH 2 and 7.4 (2.3 g/mL, 4 orders of magnitude higher than the 0.23 mg/mL of **1**). Since **9k** shows as well a high permeability in Caco-2 cells³¹ (515 nm/s), it will be undoubtedly classified as a biopharmaceutics classification system (BCS) class I compound. The BCS differentiates drugs on the basis of their solubility and permeability, allowing the prediction of drug absorption.³² The system divides drugs into four classes: I, high solubility and permeability; II, low solubility and high permeability; III, high solubility and low permeability; and IV, low solubility and low permeability. In the BCS, a drug is considered highly soluble when the highest

dose strength is soluble in 250 mL or less of aqueous media (initial gastric volume) over the pH range of 1–7.5. The compound **9k** is predicted to be class I and therefore well absorbed even at doses well above the gram.

The compound **9k** also complies with Lipinski's rules and shows moderate basicity (pK_a 6.4), an interesting attribute to comply with the central nervous system multiparameter optimization (CNS MPO) algorithm.³³ An MPO value of 6.0 was calculated for **9k**, which is the highest possible score, predicting good ADME and safety properties for CNS-directed drugs.

The compound **9k** was shown to be devoid of potential for drug–drug interactions based on both direct and time-dependent CYP inhibition for CYP1A2, 2C9, 2C19, 2D6, and 3A4 in human liver microsomes, where it showed a IC_{50} of between 100 and 1000 μM . Studies of **9k** with HepaRG cells revealed no CYP induction at concentrations 50 μM ³¹ and adequate in vitro metabolic stability in human, rat, and mouse liver microsomes.³¹ It showed as well a good in vitro safety, with lack of cytotoxic potential in the MTT (3-(4,5-dimethylthiazol-2-yl)-2,5-diphenyltetrazolium bromide) and neutral red uptake assays when tested up to 100 μM in HepG2 cells³⁴ and lack of genotoxic potential in the SOS/umu and Ames bacterial mutation assays.³⁵ Finally, **9k** can be considered as highly selective because it did not show any significant affinity for another 180 molecular targets (inhibition at 1 μM below 50% in a set of receptors, transporters, ion channels, and enzymes), indicating that the relevant in vivo activity shown below is only due to σ_1R binding. The summary in vitro profile of **9k** is shown in Figure 2.

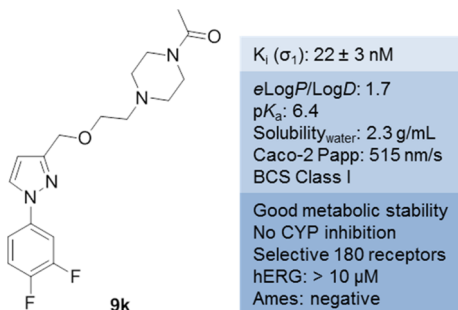


Figure 2. Structure and relevant in vitro data of the clinical candidate 9k.

The pharmacokinetic profile of **9k** was determined in mice and rats after oral and intravenous administration of single doses of 10 and 1 mg/kg, respectively, and comparative data versus **1** are outlined in Table 2. Bioavailability (*F*) was higher than 60% in both species and peak plasma concentrations

(C_{max}) after po administration were relatively high: 1178 ng/mL in rats and 771 ng/mL in mice. Total plasma clearances were high, 70% of liver blood flow in rats and 89% in mice. The volumes of distribution were higher than the total body water, 1.2 L/kg in rat and 4.4 L/kg in mice. Marked species differences were observed in elimination half-lives, with mean values of <1 and 3.4 h in rats and mice, respectively. It can be concluded that **9k** shows lower metabolic clearance than **1**, which results in higher in vivo exposure (AUCs: 1.5-fold and sixfold higher in mice and rats, respectively) and better bioavailability (Fs: twofold and fourfold higher in mice and rats, respectively).

The functional activity of **9k** was evaluated using the phenytoin assay,³⁶ where σ_1 R agonists are shifted by the allosteric ligand to significantly higher affinities (K_i ratios without phenytoin vs with phenytoin > 1), while σ_1 R antagonists show small or no shift to lower affinity values (K_i ratios without phenytoin vs with phenytoin ≤ 1). The behavior of the compound **9k** may be considered indicative of σ_1 R antagonism (K_i without phenytoin/ K_i with phenytoin = 0.9 ± 0.2). Although this value is not completely conclusive, the antagonist nature of **9k** is confirmed by its in vivo analgesia, as shown below.

The compound **9k** showed *in vivo* efficacy after oral administration in two different pain models in mice: intraplantar capsaicin-induced mechanical hypersensitivity³⁷ and partial sciatic nerve ligation (PSNL)-induced mechanical hypersensitivity,³⁸ a model representative of neuropathic pain. In the capsaicin test, the antiallodynic potency of **9k** was similar to that of the compound **1** (ED₅₀ 33 vs 28 mg/kg, respectively, [Figure 3](#), [Table 2](#)). In the PSNL model, oral administration of **9k** at 80 mg/kg, revealed an increased antiallodynic efficacy when comparing with the same dose of the compound **1** (95% vs 54%, respectively).

CONCLUSIONS

In summary, we have described the synthesis and pharmacological activity of a new series of potent and selective σ_1 R ligands. Several compounds in this family of arylpyrazoles exhibited high in vitro affinity and selectivity versus σ_2 R/TMEM97 and low potential for cardiac toxicity. The most promising compound **9k** (EST64454) behaves as a σ_1 R antagonist and shows a remarkable physicochemical profile, with a very high aqueous solubility at any physiologically meaningful pH, which in view of its high permeability in Caco-2 cells, will allow its classification as a BCS class I compound at any dose range. It also shows high metabolic stability in all species and an adequate pharmacokinetic profile in rodents. This adequate drug metabolism and pharmacokinetic (DMPK) profile, together with its in vivo antinociceptive properties in

Table 2. In Vivo Comparative Data for Compounds 9k and 1

comp	capsaicin ^a ED ₅₀ (95% CI) (mg/kg, po)	PSNL ^b efficacy ± SEM (% at 80 mg/kg, po)	mouse pharmacokinetics ^c 10 mg/kg, po						rat pharmacokinetics ^d 10 mg/kg, po					
			C _{max} (ng/mL)	t _{1/2} (h)	AUC _{0-∞} (ng·h/mL)	Cl (% LBF)	V _{ss} (l/kg)	F (%)	C _{max} (ng/mL)	t _{1/2} (h)	AUC _{0-∞} (ng·h/mL)	Cl (% LBF)	V _{ss} (l/kg)	F (%)
9k	33 (32–35)	95 ± 21	771	3.4	1431	89	4.4	69	1178	<1	2645	70	1.2	60
1	28 (20–41)	54 ± 13	622	0.7	958	65	2.2	34	301	1.2	428	109	2.9	15

^aReduction in mechanical hypersensitivity after po administration of test compounds in the mouse capsaicin test. ^bReduction in mechanical hypersensitivity after po administration of test compounds in the mouse PSNL model. ^cMouse pharmacokinetic parameters calculated as described in the [Experimental Section](#). ^dRat pharmacokinetic parameters calculated as described in the [Experimental Section](#).

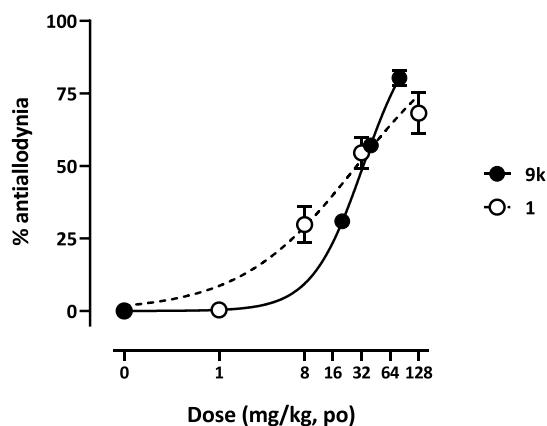


Figure 3. Dose–response effect of **9k** and **1** on the capsaicin-induced mechanical hypersensitivity test in mice. Each point and vertical line represent the mean \pm SEM of the values obtained in 8 (compound **9k**) or 8–31 (compound **1**) animals.

different animal models, prompted us to select the compound **9k** as a clinical candidate for the treatment of pain.

EXPERIMENTAL SECTION

Unless otherwise noted, all materials were obtained from commercial suppliers and used without further purification. The reference compound E-52862 (**1**) was obtained as previously described⁸ and (+)-pentazocine, haloperidol, and [³H]-Di-*o*-tolylguanidine (DTG) were commercially available. Flash chromatography was performed on a Teledyne Isco CombiFlash RF system with disposable columns. ¹H NMR and ¹³C NMR spectra were recorded on a Agilent Mercury 300 or 400 MHz (spectrometer fitted with a 5 mm ATB 1H/19F/X probe) with a 2 H lock in deuterated solvents. Chemical shifts (δ) are in parts per million. Commercially available reagents and solvents [high-performance liquid chromatography (HPLC) grade] were used without further purification for all the analytical tests. Analytical HPLC-MS for all final compounds and intermediates was performed on an Agilent HP1200-MS 6110 system. A reverse-phase XBridge C18 XP column was used (4.6 \times 30 mm, 2.5 μ m), gradient 5–100% B (A = 10 mM ammonium bicarbonate, B = acetonitrile) over 8 min, injection volume: 1 μ L, flow: 2.0 mL/min, and temperature: 40 $^{\circ}$ C. UV spectra were recorded at 210 nm using an Agilent HP1200 VWD detector. Mass spectra were obtained over the range m/z 50–1000 by electron spray ionization (ESI) in the positive mode using an Agilent MS6110 simple quadrupole. Data were integrated and reported using Agilent ChemStation software. All final compounds displayed purity equal or higher than 95%, as determined by said methods. Accurate mass measurements were carried out using an Agilent 6540 UHD Accurate-Mass QTOF system and obtained by ESI in the positive mode. Chiral analytical and preparative HPLC was performed in Agilent 1100 analytical and preparative HPLC systems, respectively. The coated or immobilized polysaccharide columns were acquired from Chiral Technologies Europe; heptane and ethanol or IPA with or without DEA at variable proportions was used as a mobile phase. All compounds active in biological assays were electronically filtered for structural attributes common to pan-assay interference compounds and were found to be negative.³⁹

Determination of Physicochemical Properties. pK_a was calculated using ACDLABS 9.0.3 and $\log P$ was calculated using ChemDraw Ultra 10.0.3. Thermodynamic solubility was measured by HPLC after stirring the solid compound for 24 h in phosphate buffer at pH = 7.4. $\log P$ and pK_a were determined using a pHmetric technique⁴⁰ in a GlpKa or Sirius-T3 analytical instrument.

General Procedures for the Synthesis of 3-(Ethoxycarbonyl)-pyrazole Derivatives 4. Ethyl 1-(3,4-Dichlorophenyl)-5-methyl-1H-pyrazole-3-carboxylate (**4a**, R^1 = 3,4-Dichlorophenyl, R^2 = Me). To a suspension of 3,4-dichlorophenyl hydrazine hydrochloride (**2**) (100 mg, 0.47 mmol) in AcOH (5 mL), ethyl acetopyruvate (**3**)

(74 mg, 0.47 mmol) was added and the mixture was stirred at 120 $^{\circ}$ C for 1 h. After this time, dichloromethane (DCM) was added and the organic layer was washed with H₂O, 10% aqueous NaOH, and brine. The organic phase was dried over Na₂SO₄, filtered, and concentrated to dryness. The residue was purified by flash chromatography (SiO₂, hexane/EtOAc 80:20) to give the compound **4a** as an orange solid (139 mg, 99%). ¹H NMR (250 MHz, CDCl₃): δ 7.62 (d, J = 2.4 Hz, 1H), 7.54 (d, J = 8.3 Hz, 1H), 7.32 (dd, J = 2.4, 8.3 Hz, 1H), 6.72 (s, 1H), 4.39 (c, J = 6.8 Hz, 2H), 2.34 (s, 3H), 1.39 (t, J = 6.8 Hz, 3H).

Ethyl 1-(3,4-Dichlorophenyl)-1H-pyrazole-3-carboxylate (4b**, R^1 = 3,4-Dichlorophenyl, R^2 = H).** To a solution of ethyl 2-chloroacetate (**6**) (1.52 g, 9.26 mmol) and NaOAc (2.41 g, 29.4 mmol) in EtOH (5 mL) at 0 $^{\circ}$ C, 3,4-dichlorobenzediazonium chloride (**5**) (1.88 g, 9.26 mmol) was added and the mixture was stirred at 0 $^{\circ}$ C for 2 h. After this time, the suspension was filtered and the solid was washed with EtOH. The obtained solid was dried and dissolved in toluene (20 mL). Then, bicyclo[2.2.1]hepta-2,5-diene (**2.06** mL, 20.31 mmol) and Et₃N (2.64 mL, 18.96 mmol) were added and the mixture was stirred at 80 $^{\circ}$ C for 2 h. The suspension was filtered again; the solid was dissolved in xylenes (20 mL) and heated to 140 $^{\circ}$ C for 16 h more. The reaction mixture was concentrated to dryness and the residue was purified by flash chromatography (SiO₂, hexane/EtOAc 100:0 to 85:15) to give the compound **4b** as a white solid (1.28 g, 66%). ¹H NMR (250 MHz, CDCl₃): δ 7.92 (m, 2H), 7.63–7.52 (m, 2H), 7.01 (d, J = 2.5 Hz, 1H), 4.45 (q, J = 7.1 Hz, 2H), 1.43 (t, J = 7.1 Hz, 3H).

General Procedure for the Synthesis of 3-(Hydroxymethyl)-pyrazole Derivatives 7. 1-(3,4-Dichlorophenyl)-5-methyl-1H-pyrazol-3-yl)methanol (**7a**). To a suspension of **4a** (551 mg, 1.84 mmol) in EtOH (12 mL), NaBH₄ (208 mg, 5.5 mmol) was added in portions and the mixture was stirred at 80 $^{\circ}$ C for 5 h. After this time, H₂O was added, and the mixture was extracted with DCM. The combined organic layers were washed with aqueous sat NH₄Cl, dried over Na₂SO₄, filtered, and concentrated to dryness. The residue was purified by flash chromatography (SiO₂, hexane/EtOAc 60:40) to give the compound **7a** as a yellow solid (354 mg, 75%). ¹H NMR (250 MHz, CDCl₃): δ 7.82 (d, J = 2.5 Hz, 1H), 7.75 (d, J = 8.5 Hz, 1H), 7.52 (m, 1H), 6.43 (s, 1H), 4.91 (s, 2H), 2.57 (s, 3H).

General Procedure for the Synthesis of 3-Methoxyalkylamine-pyrazole Derivatives 9. 4-(2-((1-(3,4-Dichlorophenyl)-5-methyl-1H-pyrazol-3-yl)methoxy)ethyl)morpholine (**9b**). To a solution of **7a** (80 mg, 0.31 mmol) in THF (3 mL), NaH (60% in mineral oil, 25 mg, 0.62 mmol) was added in portions and the mixture was stirred at rt for 5 min. Then, a solution of 4-(2-iodoethyl)-morpholine (225 mg, 0.93 mmol) in THF (2 mL) was added, and the mixture was stirred at 70 $^{\circ}$ C for 2 h. After this time, aqueous sat NaHCO₃ was added and the mixture was extracted with DCM. The combined organic layers were washed with aqueous sat NaHCO₃ and H₂O, dried over Na₂SO₄, filtered, and concentrated to dryness. The residue was purified by flash chromatography (SiO₂, DCM/MeOH 96:4) to give the compound **9b** as a white solid (114 mg, 99%). ¹H NMR (250 MHz, CDCl₃): δ 7.59 (d, J = 2.5 Hz, 1H), 7.52 (d, J = 8.6 Hz, 1H), 7.32–7.27 (dd, J = 2.5, 8.6 Hz, 1H), 6.24 (s, 1H), 4.54 (s, 2H), 3.73 (t, J = 4.6 Hz, 4H), 3.65 (t, J = 5.8 Hz, 2H), 2.62 (t, J = 5.8 Hz, 2H), 2.51 (t, J = 4.6 Hz, 4H), 2.35 (s, 3H). ¹³C NMR (101 MHz, CDCl₃): δ 150.94, 140.18, 139.08, 133.25, 131.72, 130.79, 126.61, 123.72, 107.37, 67.59, 67.00, 66.86, 58.41, 54.15, 12.77. HPLC-MS: purity 98%. HRMS [M + H]⁺ (diff ppm) 369.1015 (1.04).

1-(2-((1-(3,4-Dichlorophenyl)-5-methyl-1H-pyrazol-3-yl)-methoxy)ethyl)piperazine (**9i**). A solution of **9b** (115 mg, 0.28 mmol) in 48% HBr in AcOH (7 mL) was heated at 110 $^{\circ}$ C during 2 h. The solution was cooled to 0 $^{\circ}$ C, and a 6 M aqueous NaOH solution was added dropwise until pH = 8–9. The mixture was extracted with DCM. The combined organic layers were dried over Na₂SO₄, filtered, and concentrated to dryness. The residue was purified by flash chromatography (SiO₂, DCM/MeOH/NH₄OH 95:4:1) to give the compound **9i** as a yellow oil (88 mg, 85%). ¹H NMR (400 MHz, CDCl₃): δ 7.60 (dd, J = 0.3, 2.5 Hz, 1H), 7.52 (dd, J = 0.3, 8.6 Hz, 1H), 7.30 (dd, J = 2.5, 8.6 Hz, 1H), 6.24 (q, J = 0.8 Hz, 1H), 4.54 (s, 2H), 3.64 (t, J = 5.9 Hz, 2H), 2.89 (t, J = 4.9 Hz,

4H), 2.60 (t, $J = 5.9$ Hz, 2H), 2.54–2.39 (m, 4H), 2.35 (d, $J = 0.8$ Hz, 3H). ^{13}C NMR (101 MHz, CD_3OD): δ 151.03, 140.14, 139.10, 133.23, 131.69, 130.78, 126.61, 123.73, 107.39, 67.79, 66.84, 58.61, 55.07, 46.04, 12.77. HPLC-MS: purity 97%. HRMS $[\text{M} + \text{H}]^+$ (diff ppm) 368.1167 (−0.96).

4-(3-(1-(3,4-Dichlorophenyl)-5-methyl-1H-pyrazol-3-yl)propyl)morpholine (13a). Step 1: To a solution of **7a** (542 mg, 2.11 mmol) in DCM (30 mL), MnO_2 (2.16 g, 21.1 mmol) was added and the mixture was stirred at 40 °C for 16 h. The mixture was cooled to rt, filtered through Celite and concentrated to dryness. The residue was purified by flash chromatography (SiO_2 , hexane/EtOAc 80:20) to give 1-(3,4-dichlorophenyl)-5-methyl-1H-pyrazole-3-carbaldehyde (**10a**) as a yellow solid (403 mg, 75%). ^1H NMR (250 MHz, CDCl_3): δ 9.98 (s, 1H), 7.65 (d, $J = 2.5$ Hz, 1H), 7.61 (d, $J = 8.5$ Hz, 1H), 7.36 (dd, $J = 2.5, 8.5$ Hz, 1H), 6.73 (s, 1H), 2.39 (s, 3H).

Step 2: To a solution of 4-(2-iodoethyl)morpholine (2.0 g, 8.29 mmol) in xylenes (15 mL), PPH_3 (3.26 g, 12.44 mmol) was added and the mixture was stirred at 135 °C for 16 h. The mixture was cooled to rt; toluene (8 mL) was added and it was stirred for 2 h more. The obtained solid was filtered, washed with Et_2O , and dried under vacuum to give 2-(morpholin-4-yl)ethyltriphenylphosphonium iodide (**11a**) as a white solid (3.96 g, 95%). ^1H NMR (250 MHz, CDCl_3): δ 7.93–7.83 (m, 15H), 3.84 (m, 2H), 3.29 (m, 4H), 2.59 (m, 2H), 2.30 (m, 4H).

Step 3: To a solution of **11a** (177 mg, 0.353 mmol) in THF (3 mL), KO^tBu (79 mg, 0.7 mmol) was added and the mixture was stirred at rt for 1 min. Then, a solution of **10a** (108 mg, 0.42 mmol) in THF (3 mL) was added and the mixture was stirred at rt for 1 h more. After this time, H_2O was added and the mixture was extracted with DCM. The combined organic layers were dried over Na_2SO_4 , filtered, and concentrated to dryness. The residue was purified by two consecutive flash chromatography purifications (SiO_2 , hexane/EtOAc 50:50 and DCM/MeOH/ NH_4OH 98:2:1) to give 4-(3-(1-(3,4-dichlorophenyl)-5-methyl-1H-pyrazol-3-yl)allyl)morpholine (**12a**) as a yellow oil (45 mg, 36%). ^1H NMR (250 MHz, CDCl_3): δ (major isomer) 7.62 (d, $J = 2.5$ Hz, 1H), 7.54 (d, $J = 8.5$ Hz, 1H), 7.33 (dd, $J = 2.5, 8.5$ Hz, 1H), 6.45 (d, $J = 11.8$ Hz, 1H), 6.22 (s, 1H), 5.84 (m, 1H), 3.74 (m, 4H), 3.46 (dd, $J = 1.9, 6.3$ Hz, 2H), 2.53 (m, 4H), 2.37 (s, 3H).

Step 4: To a solution of **12a** (123 mg, 0.35 mmol) in MeOH (4 mL), PtO_2 (4 mg, 0.017 mmol) was added and the solution was stirred under a H_2 atmosphere during 2 h. After this time, the mixture was filtered through Celite and concentrated to dryness. The residue was purified by flash chromatography (SiO_2 , hexane/acetone 60:40) to give **13a** as a yellow solid (79 mg, 64%). ^1H NMR (250 MHz, CDCl_3): δ 7.59 (d, $J = 2.5$ Hz, 1H), 7.50 (d, $J = 8.8$ Hz, 1H), 7.29 (dd, $J = 2.5, 8.8$ Hz, 1H), 6.02 (s, 1H), 3.72 (m, 4H), 2.64 (t, $J = 7.7$ Hz, 2H), 2.44 (m, 6H), 2.32 (s, 3H), 1.87 (m, 2H). ^{13}C NMR (101 MHz, CDCl_3): δ 154.04, 139.60, 139.36, 133.15, 131.20, 130.71, 126.39, 123.51, 107.00, 67.16, 58.72, 53.89, 26.55, 26.20, 12.80. HPLC-MS: purity 96%. HRMS $[\text{M} + \text{H}]^+$ (diff ppm) 353.1071 (2.62).

1-(4-(3-(1-(3,4-Dichlorophenyl)-5-methyl-1H-pyrazol-3-yl)-methoxy)propyl)piperazin-1-yl)ethanone (15). Step 1: A mixture of **7a** (100 mg, 0.39 mmol), $\text{Bu}_4\text{NSO}_4\text{H}$ (6 mg, 0.02 mmol), and 1-bromo-3-chloropropane (0.09 mL, 0.97 mmol) in 40% aqueous NaOH (0.5 mL) and toluene (0.5 mL) was vigorously stirred at rt for 20 h. After this time, H_2O was added and the mixture was extracted with DCM. The combined organic layers were dried over Na_2SO_4 , filtered, and concentrated to dryness. The residue was purified by flash chromatography (SiO_2 , hexane/EtOAc 90:10) to give 3-((3-chloropropoxy)methyl)-1-(3,4-dichlorophenyl)-5-methyl-1H-pyrazole (**14**) as a yellow oil (78 mg, 56%). ^1H NMR (250 MHz, CDCl_3): δ 7.61 (d, $J = 2.5$ Hz, 1H), 7.57–7.50 (d, $J = 8.7$ Hz, 1H), 7.31 (dd, $J = 8.7, 2.5$ Hz, 1H), 6.25 (s, 1H), 4.52 (s, 2H), 3.66 (m, 4H), 2.35 (s, 3H), 2.06 (m, 2H).

Step 2: To a solution of 1-acetypiperazine (29 mg, 0.22 mmol) in DMF (5 mL), DIPEA was added (0.11 mL, 0.67 mmol) and the mixture was stirred at rt for 15 min. Then, a solution of **14** (75 mg, 0.22 mmol) and NaI (50 mg, 0.33 mmol) in DMF (2 mL) was added

and the mixture was stirred at 90 °C for 3 h. After this time, the reaction mixture was concentrated to dryness and the residue was purified by flash chromatography (SiO_2 , DCM/MeOH 100:0 to 93:7) to give the compound **15** as a yellow oil (45 mg, 47%). ^1H NMR (400 MHz, CDCl_3): δ 7.60 (dd, $J = 0.3, 2.5$ Hz, 1H), 7.52 (dd, $J = 0.3, 8.6$ Hz, 1H), 7.30 (dd, $J = 2.5, 8.6$ Hz, 1H), 6.24 (q, $J = 0.8$ Hz, 1H), 4.50 (s, 2H), 3.62–3.59 (m, 2H), 3.57 (t, $J = 6.5$ Hz, 2H), 3.47–3.42 (m, 2H), 2.50–2.37 (m, 6H), 2.35 (d, $J = 0.8$ Hz, 3H), 2.08 (s, 3H), 1.81 (ddt, $J = 6.4, 7.3, 8.7$ Hz, 2H). ^{13}C NMR (101 MHz, CD_3OD): δ 169.04, 151.06, 140.14, 139.09, 133.24, 131.72, 130.78, 126.62, 123.72, 107.34, 68.95, 66.73, 55.43, 53.44, 52.92, 46.43, 41.54, 27.18, 21.49, 12.77. HPLC-MS: purity 97%. HRMS $[\text{M} + \text{H}]^+$ (diff ppm) 424.1438 (1.3).

1-(4-(2-((1-(3,4-Difluorophenyl)-1H-pyrazol-3-yl)methoxy)ethyl)piperazin-1-yl)ethanone Hydrochloride (9k, Scheme 2 Method). Step 1: To a solution of ethyl 1H-pyrazole-3-carboxylate (**16**) (31.0 g, 221.2 mmol), CuI (8.42 g, 44.2 mmol) and Cs_2CO_3 (144 g, 441.9 mmol) in MeCN (310 mL), 1,2-difluoro-4-iodobenzene (**17**) (71.6 g, 298.3 mmol), and TMEDA (13.35 mL, 88.5 mmol) were added and the mixture was stirred at 85 °C for 6 h. After this time, the mixture was cooled to rt and the formed salts were filtered and washed with MeCN. The filtered salts were dissolved in H_2O and the remaining MeCN was removed under vacuum. The suspension was stirred at rt during 1 h and was filtered again washing with H_2O . The obtained solid was dried under vacuum to give a 97:3 mixture of ethyl 1-(3,4-difluorophenyl)-1H-pyrazole-3-carboxylate (**18**) and ethyl 1-(3,4-difluorophenyl)-1H-pyrazole-5-carboxylate (**19**) as a white solid (44.8 g, 80%). ^1H NMR (250 MHz, CDCl_3): δ (major isomer) 7.87 (d, $J = 2.5$ Hz, 1H), 7.66 (ddd, $J = 10.8, 6.9, 2.7$ Hz, 1H), 7.50–7.41 (m, 1H), 7.32–7.20 (m, 1H), 6.99 (d, $J = 2.5$ Hz, 1H), 4.43 (q, $J = 7.1$ Hz, 2H), 1.42 (t, $J = 7.1$ Hz, 3H).

Step 2: To a solution of a 97:3 mixture of **18** and **19** (33.5 g, 133.0 mmol) in THF (160 mL) under a nitrogen atmosphere, a 2 M solution of LiBH_4 in THF (66.5 mL, 133.0 mmol) was added and the reaction mixture was stirred at 70 °C for 4 h. After cooling to rt, H_2O (200 mL) and 10% aqueous HCl were added until pH = 4–5. Then, 20% aqueous NaOH was added until pH = 6–7 and half of the initial volume was removed under vacuum. The suspension was stirred at rt for 1 h and was filtered washing with H_2O . The obtained solid was dried under vacuum to give 1-(3,4-difluorophenyl)-1H-pyrazol-3-yl)methanol (**20**) as a white solid (27.4 g, 98%). ^1H NMR (250 MHz, CDCl_3): δ 7.80 (d, $J = 2.2$ Hz, 1H), 7.54 (ddd, $J = 11.1, 7.0, 2.6$ Hz, 1H), 7.40–7.30 (m, 1H), 7.29–7.16 (m, 1H), 6.46 (d, $J = 2.2$ Hz, 1H), 4.76 (d, $J = 5.1$ Hz, 2H), 2.38 (t, $J = 5.1$ Hz, 1H).

Step 3: To a solution of **20** (27.4 g, 130.2 mmol) in THF (130 mL), KOH (36.53 g, 651.1 mmol) was added. Then, a solution of TsCl (32.3 g, 169.3 mmol) in THF (130 mL) was slowly added and the reaction was stirred for 2 h. H_2O was added and it was extracted with EtOAc. The combined organic phases were washed with H_2O , dried over Na_2SO_4 , filtered, and concentrated to dryness obtaining a brown solid that was triturated with hexane and filtered to give 1-(3,4-difluorophenyl)-1H-pyrazol-3-yl)methyl 4-methylbenzenesulfonate (**21**) as a white solid (42.4 g, 89%). ^1H NMR (250 MHz, CDCl_3): δ 7.80 (d, $J = 8.2$ Hz, 2H), 7.76 (d, $J = 2.4$ Hz, 1H), 7.56 (ddd, $J = 11.2, 6.6, 2.2$ Hz, 1H), 7.34–7.17 (m, 4H), 6.46 (d, $J = 2.7$ Hz, 1H), 5.14 (s, 2H), 2.43 (s, 3H).

Steps 4 and 5: To a suspension of NaH (60%, 2.64 g, 66.0 mmol) in THF (200 mL), 1-(4-(2-hydroxyethyl)piperazin-1-yl)ethanone hydrochloride (**22**) (11.3 g, 65.8 mmol) was added in portions and the suspension was stirred for 30 min. Then, **21** (20.0 g, 54.9 mmol) was added in portions and the reaction mixture was stirred at rt for 3 h. After this time, H_2O (200 mL) and 37% aqueous HCl were added until pH = 7–7.5; excess THF was removed under vacuum and 37% aqueous HCl was again added until pH = 2–3. The aqueous phase was washed with EtOAc and 20% aqueous NaOH was added until pH = 8.5–10. The aqueous phase was then extracted with EtOAc. The combined organic phases were concentrated to dryness to afford the free base of **9k**. Methyl ethyl ketone was added and the solution was heated to 50 °C. A 5 M solution of HCl in IPA (11 mL, 55 mmol) was added and the solution was left to crystallize at 0 °C; the obtained

solid was filtered and dried under vacuum to give **9k** as a white solid (16.7 g, 76%). mp 155–157 °C; ^1H NMR (250 MHz, CDCl_3): δ 13.14 (bs, 1H), 7.82 (d, J = 2.5 Hz, 1H), 7.55 (ddd, J = 11.1, 6.9, 2.5 Hz, 1H), 7.42–7.32 (m, 1H), 7.31–7.17 (m, 1H), 6.46 (d, J = 2.5 Hz, 1H), 4.68 (s, 1H), 4.62 (s, 2H), 4.17–4.04 (m, 3H), 3.91–3.39 (m, 4H), 3.27 (s, 2H), 2.87 (s, 2H), 2.09 (s, 3H). ^{13}C NMR (101 MHz, CD_3OD): δ 171.76, 152.43, 151.83 (dd, J = 13.7, 247.6 Hz), 150.06 (dd, J = 12.7, 246.5 Hz), 138.05 (dd, J = 3.0, 5.3 Hz), 130.42, 119.23 (d, J = 18.8 Hz), 116.21 (dd, J = 3.7, 6.4 Hz), 109.90 (d, J = 22.0 Hz), 108.98, 67.43, 64.23, 57.42, 52.98, 52.78, 44.04, 39.28, 20.88. HPLC-MS: purity 97%. HRMS $[\text{M} + \text{H}]^+$ (diff ppm) 364.1717 (1.67).

Human Sigma-1 Receptor Radioligand Assay.⁸ The binding properties of the test compounds to human $\sigma_1\text{R}$ were studied in transfected HEK-293 membranes using $[\text{^3H}](+)\text{-pentazocine}$ (PerkinElmer, NET-1056) as the radioligand. The assay was carried out with 7 μg of membrane suspension, $[\text{^3H}](+)\text{-pentazocine}$ (5 nM, 100 μL), in either the absence or presence of either buffer or 10 μM haloperidol for total and nonspecific binding, respectively. Binding buffer contained Tris-HCl (50 mM, at pH 8). Plates were incubated at 37 °C for 120 min. After the incubation period, the reaction mix was transferred to MultiScreen HTS, FC plates (Millipore) presoaked in 100 μL of 0.1% polyethyleneimine and filtered. Then, plates were washed (three times) with ice-cold Tris-HCl (10 mM, pH 7.4). Filters were dried and counted at approximately 40% efficiency in a MicroBeta scintillation counter (PerkinElmer) using an EcoScint liquid scintillation cocktail.

Guinea Pig Sigma-2 Receptor Radioligand Assay. The binding properties of test compounds to guinea pig $\sigma_2\text{R}$ were studied in guinea pig brain membranes as described¹³ with some modifications. DTG (PerkinElmer, Code NET-986) was used as the radioligand. The assay was carried out with 200 μg of membrane suspension, $[\text{^3H}]\text{-DTG}$ (10 nM), in either the absence or presence of either buffer or 10 μM haloperidol for total and nonspecific binding, respectively. Binding buffer contained Tris-HCl (50 mM, pH 8) and $\sigma_1\text{R}$ was blocked with (+)-SKF10047 at 400 nM. Plates were incubated at 25 °C for 120 min. After the incubation period, the reaction mixture was transferred to MultiScreen HTS, FC plates (Millipore) and filtered and plates were washed three times with ice-cold 50 mM Tris-HCl (pH 7.4). Filters were dried and counted at approximately 40% efficiency in a MicroBeta scintillation counter (PerkinElmer) using an EcoScint liquid scintillation cocktail.

hERG Assay.²⁹ CHO cells stably expressing hERG channels (Millipore) were cultured in F12 HAM medium supplemented with 10% FBS and 400 $\mu\text{g}/\text{L}$ Geneticin. Extracellular Ringer's solution consisted of (in mM) 2 CaCl_2 , 1 MgCl_2 , 10 HEPES, 4 KCl, 145 NaCl, and 10 glucose with pH 7.4 and 305 mOsm. Intracellular Ringer's solution consisted of (in mM) 5.37 CaCl_2 , 1.75 MgCl_2 , 31.25/10 KOH/EGTA, 10 HEPES, and 210 KCl with pH 7.2 and 295 mOsm. $\text{Na}_2\text{-ATP}$ (4 mM) was added to intracellular Ringer's solution shortly before use. Whole-cell currents were measured with a QPatch system (Sophion) in response to continuously executed voltage protocols as per the manufacturer's recommendations. Upon the onset of the voltage protocol, cells were maintained at a holding potential (V_h) of -80 mV, then clamped briefly to -50 mV (20 ms), subsequently depolarized to 20 mV for 4800 ms, and finally repolarized to -50 mV for 5000 ms, at which potential the peak outward tail current was measured. Finally, the voltage returned to V_h for 3100 ms. Thus, voltage protocols were repeated for each 15 s. For each cell, the extracellular solution was applied previously to increasing concentrations of the tested compound.

In Vivo Studies. The experimental detail of capsaicin and PSLN models is given in the Supporting Information. All animal research was conducted in accordance with protocols approved by the local Committee of Animal Use and Care, with the Care and Use of Laboratory Animals Guidelines of the European Community (European Directive 2010/63/EU), and with the International Association for the Study of Pain Guidelines on ethical standards for investigation in animals.⁴¹ Animal studies are reported in compliance with the ARRIVE guidelines.^{42,43}

Pharmacokinetic Studies. Groups of two male Wistar rats (250–300 g; Harlan) or 16 male CD1 mice (25–30 g; Charles River) were given oral or intravenous doses of **9k** and **1** in 0.5% hydroxypropyl methylcellulose or saline solution, respectively. Dose levels were 10 mg/kg for oral studies and 1 mg/kg for intravenous studies. Blood samples were collected at different times from the saphenous vein or by intracardiac puncture into heparinized tubes. Plasma was obtained by blood centrifugation at 4 °C and 2280g for 10 min and kept at -80 °C until analysis. Plasma samples were assayed by high-performance liquid chromatography–triple quadrupole mass spectrometry (HPLC-MS/MS) after plasma protein precipitation.

Pharmacokinetic Parameters. Standard pharmacokinetic parameters, such as the area under the curve (AUC), peak plasma concentration (C_{max}), time to peak concentration (t_{max}), oral bioavailability (F), total plasma clearance (Cl), volume of distribution at the steady state (V_{ss}), and terminal half-life ($t_{1/2}$), were determined by noncompartmental analysis of the plasma concentration–time curves (Phoenix v.6.2.1.51, Pharsight, CA).

■ ASSOCIATED CONTENT

Supporting Information

The Supporting Information is available free of charge at <https://pubs.acs.org/doi/10.1021/acs.jmedchem.0c01575>.

Analytical data for all the final compounds and intermediates. HPLC traces for final compounds of formula 9, 13, and 15. Experimental description of in vivo studies (PDF)

Molecular Formula Strings (CSV)

■ AUTHOR INFORMATION

Corresponding Author

Carmen Almansa – ESTEVE Pharmaceuticals, Torre Esteve, 08038 Barcelona, Spain; orcid.org/0000-0001-5665-4685; Phone: 0034650697372; Email: calmansa@welab.barcelona

Authors

José Luis Díaz – ESTEVE Pharmaceuticals, Torre Esteve, 08038 Barcelona, Spain; orcid.org/0000-0001-8812-4689

Mónica García – ESTEVE Pharmaceuticals, Torre Esteve, 08038 Barcelona, Spain

Antoni Torrens – ESTEVE Pharmaceuticals, Torre Esteve, 08038 Barcelona, Spain

Ana María Caamaño – Galchimia, S.A., 15823 O Pino, A Coruña, Spain

Juan Enjo – Galchimia, S.A., 15823 O Pino, A Coruña, Spain

Cristina Sicre – Galchimia, S.A., 15823 O Pino, A Coruña, Spain

Adriana Lorente – ESTEVE Pharmaceuticals, Torre Esteve, 08038 Barcelona, Spain

Adriana Port – ESTEVE Pharmaceuticals, Torre Esteve, 08038 Barcelona, Spain

Ana Montero – ESTEVE Pharmaceuticals, Torre Esteve, 08038 Barcelona, Spain

Sandra Yeste – ESTEVE Pharmaceuticals, Torre Esteve, 08038 Barcelona, Spain

Inés Álvarez – ESTEVE Pharmaceuticals, Torre Esteve, 08038 Barcelona, Spain

Miquel Martín – Laboratory of Neuropharmacology, Facultat de Ciències de la Salut i de la Vida, Universitat Pompeu Fabra, 08003 Barcelona, Spain

Rafael Maldonado – Laboratory of Neuropharmacology, Facultat de Ciències de la Salut i de la Vida, Universitat Pompeu Fabra, 08003 Barcelona, Spain

Beatriz de la Puente – ESTEVE Pharmaceuticals, Torre Esteve, 08038 Barcelona, Spain

Alba Vidal-Torres – ESTEVE Pharmaceuticals, Torre Esteve, 08038 Barcelona, Spain

Cruz Miguel Cendán – Department of Pharmacology, Faculty of Medicine, University of Granada, 18016 Granada, Spain

José Miguel Vela – ESTEVE Pharmaceuticals, Torre Esteve, 08038 Barcelona, Spain

Complete contact information is available at:

<https://pubs.acs.org/10.1021/acs.jmedchem.0c01575>

Author Contributions

The manuscript was written through contributions of all authors. All authors have given approval to the final version of the manuscript.

Notes

The authors declare no competing financial interest.

ACKNOWLEDGMENTS

We thank Ma Magdalena Bordas, Raquel Enrech, Joan Andreu Morató, Mónica Carro, Edmundo Ortega, Manel Merlos, Pilar Pérez, Javier Burgueño, Marta Pujol, Enrique Hernández, Javier Farré, Eva Ayet, Raquel Fernández-Reinoso, Maria Teresa Serafini, Carmen Segalés, Alicia Pardo, Daniel Zamanillo, and Lucía Romero for their expert contribution to analytical, in vitro, and in vivo studies and Carlos Pérez and Eduardo Villarroel for their contribution to compound management. This work was a part of activities in R&D Projects IDI-20110577 and IDI-20130942 supported by the Spanish Ministerio de Economía y Competitividad (MINECO), through the Centro para el Desarrollo Tecnológico Industrial (CDTI), cofinanced by the European Union through the European Regional Development Fund (ERDF; Fondo Europeo de Desarrollo Regional, FEDER).

ABBREVIATIONS

ADME, absorption, distribution, metabolism, and excretion; ER, endoplasmic reticulum; BCS, biopharmaceutics classification system; CNS MPO, central nervous system multi-parameter optimization; DMPK, drug metabolism and pharmacokinetics; hERG, human ether-a-go-go-related gene; PGRMC1, progesterone receptor membrane component 1; MTT, 3-(4,5-dimethylthiazol-2-yl)-2,5-diphenyltetrazolium bromide; PSNL, partial sciatic nerve ligation; SAR, structure–activity relationships; σ_1 R, sigma-1 receptor; σ_1 R-KO, sigma-1 receptor knockout mice

REFERENCES

- (1) Turk, D. C.; Wilson, H. D.; Cahana, A. Treatment of chronic non-cancer pain. *Lancet* **2011**, *377*, 2226–2235.
- (2) Goldberg, D. S.; McGee, S. J. Pain as a global public health priority. *BMC Public Health* **2011**, *11*, 770.
- (3) Zamanillo, D.; Romero, L.; Merlos, M.; Vela, J. M. Sigma 1 receptor: A new therapeutic target for pain. *Eur. J. Pharmacol.* **2013**, *716*, 78–93.
- (4) Maurice, T.; Su, T.-P. The pharmacology of sigma-1 receptors. *Pharmacol. Ther.* **2009**, *124*, 195–206.
- (5) Pasternak, G. W. Allosteric modulation of opioid G-protein coupled receptors by sigma1-receptors. *Handb. Exp. Pharmacol.* **2017**, *244*, 163.

- (6) Chien, C.-C.; Pasternak, G. W. Sigma antagonists potentiate opioid analgesia in rats. *Neurosci. Lett.* **1995**, *190*, 137–139.
- (7) Cendán, C. M.; Pujalte, J. M.; Portillo-Salido, E.; Montoliu, L.; Baeyens, J. M. Formalin-induced pain is reduced in sigma (1) receptor knockout mice. *Eur. J. Pharmacol.* **2005**, *511*, 73–74.
- (8) Díaz, J. L.; Cuberes, R.; Berrocal, J.; Contijoch, M.; Christmann, U.; Fernández, A.; Port, A.; Holenz, J.; Buschmann, H.; Laggner, C.; Serafini, M. T.; Burgueño, J.; Zamanillo, D.; Merlos, M.; Vela, J. M.; Almansa, C. Synthesis and biological evaluation of the 1-arylpyrazole class of σ_1 receptor antagonists: Identification of 4-{2-[S-methyl-1-(naphthalen-2-yl)-1H-pyrazol-3-yloxy]ethyl}morpholine (S1RA, E-52862). *J. Med. Chem.* **2012**, *55*, 8211–8224.
- (9) Bruna, J.; Videla, S.; Argyriou, A. A.; Velasco, R.; Villoria, J.; Santos, C.; Nadal, C.; Cavaletti, G.; Alberti, P.; Briani, C.; Kalofonos, H. P.; Cortinovis, D.; Sust, M.; Vaqué, A.; Klein, T.; Plata-Salamán, C. Efficacy of a novel sigma-1 receptor antagonist for oxaliplatin-induced neuropathy: A randomized, double-blind, placebo-controlled phase IIa clinical trial. *Neurotherapeutics* **2018**, *15*, 178–189.
- (10) Available from: www.clinicaltrialsregister.eu/ctr-search/trial/2011-003302-24/results (accessed 14 Nov, 2017).
- (11) Glennon, R. A.; Ablordepppey, S. Y.; Ismaiel, A. M.; El-Ashmaw, M. B.; Fischer, J. B.; Howie, K. B. Structural features important for σ_1 receptor binding. *J. Med. Chem.* **1994**, *37*, 1214–1219.
- (12) DeHaven-Hudkins, D. L.; Fleissner, L. C.; Ford-Rice, F. Y. Characterization of the binding of [3 H](+)-pentazocine to recognition sites in guinea pig brain. *Eur. J. Pharmacol.* **1992**, *227*, 371–378.
- (13) Ronsisvalle, G.; Marrazzo, A.; Prezzavento, O.; Cagnotto, A.; Mennini, T.; Parenti, C.; Scotto, G. M. Opioid and sigma receptor studies. New developments in the design of selective sigma ligands. *Pure Appl. Chem.* **2001**, *73*, 1499–1509.
- (14) (a) Hanner, M.; Moebius, F. F.; Flandorfer, A.; Knaus, H. G.; Triessnig, J.; Kempner, E.; Glossmann, H. Purification, molecular cloning, and expression of the mammalian sigma₁-binding site. *Proc. Natl. Acad. Sci. U.S.A.* **1996**, *93*, 8072–8077. (b) Kekuda, R.; Prasad, P. D.; Fei, Y.-J.; Leibach, F. H.; Ganapathy, V. Cloning and functional expression of the human type 1 sigma receptor (hSigmaR1). *Biochem. Biophys. Res. Commun.* **1996**, *229*, 553–558.
- (15) Kim, F. J.; Pasternak, G. W. Cloning the sigma2 receptor: Wandering 40 years to find an identity. *Proc. Natl. Acad. Sci. U.S.A.* **2017**, *114*, 6888–6890.
- (16) (a) Xu, J.; Zeng, C.; Chu, W.; Pan, F.; Rothfuss, J. M.; Zhang, F.; Tu, Z.; Zhou, D.; Zeng, D.; Vangveravong, S.; Johnston, F.; Spitzer, D.; Chang, K. C.; Hotchkiss, R. S.; Hawkins, W. G.; Wheeler, K. T.; Mach, R. H. Identification of the PGRMC1 protein complex as the putative sigma-2 receptor binding site. *Nat. Commun.* **2011**, *2*, 380. (b) Ahmed, I. S. A.; Chamberlain, C.; Craven, R. J. S2R (Pgrmc1): the cytochrome-related sigma-2 receptor that regulates lipid and drug metabolism and hormone signaling. *Expert Opin. Drug Metab. Toxicol.* **2012**, *8*, 361–370.
- (17) Alon, A.; Schmidt, H. R.; Wood, M. D.; Sahn, J. J.; Martin, S. F.; Kruse, A. C. Identification of the gene that codes for the σ_2 receptor. *Proc. Natl. Acad. Sci. U.S.A.* **2017**, *114*, 7160–7165.
- (18) Yalkowsky, S. H.; Valvani, S. C. Solubility and partitioning I: Solubility of nonelectrolytes in water. *J. Pharm. Sci.* **1980**, *69*, 912–922.
- (19) Díaz, J. L.; Christmann, U.; Fernández, A.; Luengo, M.; Bordas, M.; Enrech, R.; Carro, M.; Pascual, R.; Burgueño, J.; Merlos, M.; Benet-Buchholz, J.; Cerón-Bertran, J.; Ramírez, J.; Reinoso, R. F.; Fernández de Henestrosa, A. R.; Vela, J. M.; Almansa, C. Synthesis and biological evaluation of a new series of hexahydro-2H-pyrano[3,2-c]quinolines as novel selective σ_1 receptor ligands. *J. Med. Chem.* **2013**, *56*, 3656–3665.
- (20) Leeson, P. D.; Springthorpe, B. The influence of drug-like concepts on decision-making in medicinal chemistry. *Nat. Rev. Drug Discovery* **2007**, *6*, 881–890.
- (21) Hughes, J. D.; Blagg, J.; Price, D. A.; Bailey, S.; Decrescenzo, G. A.; Devraj, R. V.; Ellsworth, E.; Fobian, Y. M.; Gibbs, M. E.; Gilles, R. W.; Greene, N.; Huang, E.; Krieger-Burke, T.; Loesel, J.; Wager, T.;

Whiteley, L.; Zhang, Y. Physicochemical drug properties associated with in vivo toxicological outcomes. *Bioorg. Med. Chem. Lett.* **2008**, *18*, 4872–4875.

(22) García, M.; Torrens, A.; Díaz, J. L.; Caamaño, A. M. Pyrazole Compounds as Sigma Receptor Inhibitors. PCT Int. Appl. WO 2011147910 A1, Dec 1, 2011.

(23) Kost, A. N.; Grandberg, I. I. Progress in pyrazole chemistry. *Adv. Heterocycl. Chem.* **1966**, *6*, 347–429.

(24) Garanti, L.; Sala, A.; Zecchi, G. Synthesis of 6-oxo-2,6-dihydro-4H-furo[3,4-c]pyrazoles and 6-oxo-4H,6H-furo[3,4-c][1,2]oxazoles from 2-alkynyl acetoacetates. *Synthesis* **1975**, *1975*, 666–669.

(25) Sutherland, H. S.; Blaser, A.; Kmentova, I.; Franzblau, S. G.; Wan, B.; Wang, Y.; Ma, Z.; Palmer, B. D.; Denny, W. A.; Thompson, A. M. Synthesis and structure–activity relationships of antitubercular 2-nitroimidazooxazines bearing heterocyclic side chains. *J. Med. Chem.* **2010**, *53*, 855–866.

(26) Almansa Rosales, C.; Caamaño Roures, A. M.; Enjo Babío, J. Process and Intermediates for the Preparation of 1-(4-(2-((1-(3,4-Difluorophenyl)-1H-pyrazol-3-yl)methoxy)ethyl)piperazin-1-yl)-ethanone. PCT Int. Appl. WO 2018109082 A1, Jun 21, 2018.

(27) Bomhard, E. M.; Herbold, B. A. Genotoxic activities of aniline and its metabolites and their relationship to the carcinogenicity of aniline in the spleen of rats. *Crit. Rev. Toxicol.* **2005**, *35*, 783–835.

(28) (a) Cristau, H.-J.; Cellier, P. P.; Spindler, J.-F.; Taillefer, M. Mild conditions for copper-catalysed N-arylation of pyrazoles. *Eur. J. Org. Chem.* **2004**, *2004*, 695–709. (b) Antilla, J. C.; Baskin, J. M.; Barder, T. E.; Buchwald, S. L. Copper-diamine-catalyzed N-arylation of pyrroles, pyrazoles, indazoles, imidazoles, and triazoles. *J. Org. Chem.* **2004**, *69*, 5578–5587.

(29) Diaz, G. J.; Daniell, K.; Leitza, S. T.; Martin, R. L.; Su, Z.; McDermott, J. S.; Cox, B. F.; Gintant, G. A. The [³H]-dofetilide binding assay is a predictive screening tool for hERG blockade and proarrhythmia: Comparison of intact cell and membrane preparations and effects of altering [K⁺]_o. *J. Pharmacol. Toxicol. Methods* **2004**, *50*, 187–199.

(30) Diaz, J. L.; Christmann, U.; Fernández, A.; Torrens, A.; Port, A.; Pascual, R.; Álvarez, I.; Burgueño, J.; Monroy, X.; Montero, A.; Balada, A.; Vela, J. M.; Almansa, C. Synthesis and structure-activity relationship (SAR) study of a new series of selective σ_1 receptor ligands for the treatment of pain: 4-Aminotriazoles. *J. Med. Chem.* **2015**, *58*, 2441–2451.

(31) Yeste, S.; Reinoso, R. F.; Ayet, E.; Pretel, M. J.; Balada, A.; Serafini, M. T. Preliminary in vitro assessment of the potential of EST64454, a sigma-1 receptor antagonist, for pharmacokinetic drug-drug interactions. *Biol. Pharm. Bull.* **2020**, *43*, 68–76.

(32) Amidon, G. L.; Lennernäs, H.; Shah, V. P.; Crison, J. R. A theoretical basis for a biopharmaceutic drug classification: the correlation of in vitro drug product dissolution and in vivo bioavailability. *Pharm. Res.* **1995**, *12*, 413–420.

(33) Wager, T. T.; Hou, X.; Verhoest, P. R.; Villalobos, A. Moving beyond rules: The development of a central nervous system multiparameter optimization (CNS MPO) approach to enable alignment of drug-like properties. *ACS Chem. Neurosci.* **2010**, *1*, 435–449.

(34) Putnam, K. P.; Bombick, D. W.; Doolittle, D. J. Evaluation of eight in vitro assays for assessing the cytotoxicity of cigarette smoke condensate. *Toxicol. In Vitro* **2002**, *16*, 599–607.

(35) (a) Maron, D. M.; Ames, B. N. Revised methods for the salmonella mutagenicity test. *Mutat. Res.* **1983**, *113*, 173–215.

(b) Reifferscheid, G.; Heil, J. Validation of the SOS/umu test using test results of 486 chemicals and comparison with the Ames test and carcinogenicity data. *Mutat. Res.* **1996**, *369*, 129–145.

(36) Cobos, E. J.; Baeyens, J. M.; Del Pozo, E. Phenytoin differentially modulates the affinity of agonist and antagonist ligands for sigma 1 receptors of guinea pig brain. *Synapse* **2005**, *55*, 192–195.

(37) Entrena, J. M.; Cobos, E. J.; Nieto, F. R.; Cendán, C. M.; Gris, G.; Del Pozo, E.; Zamanillo, D.; Baeyens, J. M. Sigma-1 receptors are essential for capsaicin-induced mechanical hypersensitivity: Studies

with selective sigma-1 ligands and sigma-1 knockout mice. *Pain* **2009**, *143*, 252–261.

(38) Malmberg, A. B.; Basbaum, A. I. Partial sciatic nerve injury in the mouse as a model of neuropathic pain: Behavioral and neuroanatomical correlates. *Pain* **1998**, *76*, 215–222.

(39) Baell, J. B.; Holloway, G. A. New substructure filters for removal of pan assay interference compounds (PAINS) from screening libraries and their exclusion in bioassays. *J. Med. Chem.* **2010**, *53*, 2719–2740.

(40) Box, K.; Comer, J. Using measured pKa, logP and solubility to investigate supersaturation and predict BCS class. *Curr. Drug Metab.* **2008**, *9*, 869–878.

(41) Zimmermann, M. Ethical guidelines for investigations of experimental pain in conscious animals. *Pain* **1983**, *16*, 109–110.

(42) McGrath, J.; Drummond, G.; McLachlan, E.; Kilkenny, C.; Wainwright, C. Guidelines for reporting experiments involving animals: the ARRIVE guidelines. *Br. J. Pharmacol.* **2010**, *160*, 1573–1576.

(43) McGrath, J. C.; Lilley, E. Implementing guidelines on reporting research using animals (ARRIVE etc.): new requirements for publication in BJP. *Br. J. Pharmacol.* **2015**, *172*, 3189–3193.